Original Article

Adsorption Monitoring of Triflouroaceticacid, Pentadecyl Ester and Pentadecanoic Acid, 14-Methyl-, Methyl Ester on Fe (110): using DFT and Molecular Simulation

Abdullahi Muhammad Ayuba¹ (iD) **| Thomas Aondofa Nyijime²** (iD) **| Safiyya Abubakar Minjibir¹** (iD) **| Fater Iorhuna¹,*** (iD)

¹ *Bayero University, Department of Pure and Industrial Chemistry, Kano, 700241, Nigeria*
² *Department of Chemistry, Joseph Saawuan Tarka University Makurdi, Benue Nigeria*

ABSTRACT

Quantum functions were used to assess a theoretical investigation on mild steel's resistance to corrosion. To determine the stable geometry of the investigated compounds, TPE and PME, local density function B3LYP was optimized and simulated using DFT under restricted spin polarization DNP basis. The molecules' local and global reactivity, including their electronegativity (χ), dipole moment (μ), energy gap (ΔE), global hardness (η), global electrophilicity index (ω), energy of back donation (ΔE_{b-d}), fraction of electron transfer (ΔN), and the ($\omega+$) and ($\omega-$) electron accepting and donating powers between the molecule and the iron, were all studied. The inhibition process was assumed to be a chemisorption interaction between the surface and the molecule based on the number of adsorption sites and the binding energy obtained from the process. This is because the molecules contain hetero-atoms, such as oxygen and methylene (-CH2-) functional groups. For PME and flourine for TPE, which serve as the focal point for the selectivity of electron donation and acceptance between the metal and the TPE and PME moieties.

Introduction

Corrosion is an undesirable result of chemistry on our environment. Temperature, pressure, and acid concentration are some of the environmental factors that cause corrosion [1, 3]. Iron (Fe) is the main component of mild steel, an alloy that is occasionally used to make vehicle bodywork and a number of industrially essential components [4-8]. Given that mild steel is used in building the majority of buildings and bridges today, it is pertinent that mild steel should be protected by the corrosive environment. Other metals like Aluminum are not utilized frequently due to their high cost. One of the environmental factors acidic concentrations often used for electrochemical etching, cleaning, and pickling in the oil and gas sector [9,10] which result in the corrosion of some of the metals in question. The process also, reduces the physical

---

properties of the metals, such as luster, malleability, tension, and strain, and washes away the metals and alloys used [11].

Corrosion is the gradual deterioration of metallic materials brought on by a variety of environmental conditions such as temperature pressure and acid concentration [12,13]. Corrosion may permanently damage a material or physical properties of a metal. Numerous methods have been employed to shield metals from the factor mentioned. These methods include: interfacial potential, protective coatings, and environmental alterations but green inhibition of metals seems to be the best method. As such different method including DFT method has been employed to identify the potential of some of the compounds obtained from some green inhibitors [14].

Green inhibitors are organic compounds originating from plants that include heteropolar atoms with a single pair of electrons and unsaturated bonds S, N, O, and P [15]. Based on documented studies, these compounds have the potential to function as corrosion inhibitors hence having enough potential to bind saving as a protective surface for the metals then preventing the mentioned factors from having quick access to the metal [16,17].

To mitigate human error in techniques such as weight loss, this study employed Density Functional Theory (DFT) and Molecular Dynamic Simulation to monitor and compare the corrosion inhibition of the following esters: Triflouroacetic Acid, Pentadecyl Ester (TPE), Pentadecanoic Acid, 14-methyl-methyl ester (PME) to determine their potential effectiveness in preventing mild steel corrosion (Figure 1).
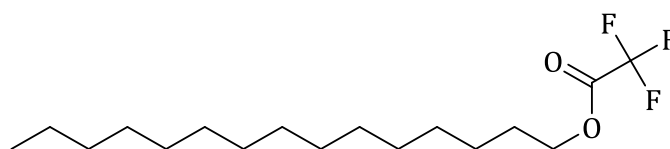
Triflouroaceticacid, pentadecyl ester
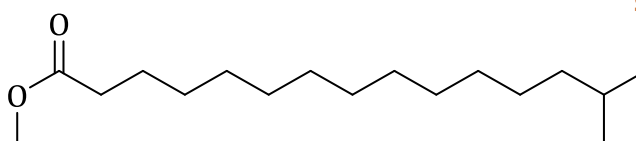
Pentadecanoic acid, 14-methyl-, methyl ester

Figure 1 the structure of the compounds used

Computational Methods

Sketching and Geometric Optimization of the Molecules

The substances under investigation were sketched using CambridgeSoft's ChemDraw Ultra 7.0.3. With the application of DMol3, the molecules' torsional and conformational energies were reduced using BIOVIA Materials Studio 8.0 (Accelrys, Inc.). The following setups were used throughout the optimization process: DNP+ basis. to constrained spin polarization in aqueous phase, the local density functional was set to B3LYP.

Quantum Chemical Parameters Calculations

Ionization potential (IP) and electron affinity (EA) are related to the energy of the frontier molecular orbital, the energy of the highest occupied molecular orbital (EHOMO), and the energy of the lowest unoccupied molecular orbital (ELUMO) in accordance with Koopman's theory [14–17] as shown in equations (2) and (3)

$$I.P = -EHOMO \qquad (1)$$

$$E.A = -ELUMO \qquad (2)$$

The dipole moment, which is equal to the magnitude of the charge (Q) at either end of the molecular dipole times the distance (r), is a measurement of net molecular polarity. The Dipole moment (μ) of the molecule can be used to determine the distribution of electrons between two linked atoms [18].

Pearson states that equation (3) provides an approximate definition for the value of global hardness (η). According to Equation 4, the system's global softness (S) is equal to its global hardness (H).

$$\eta = \frac{IE - EA}{2} \qquad (3)$$

$$S = \frac{1}{\eta} \qquad (4)$$

The relationship needed for figuring out the molecules' reaction stability is energy gap. Energy gap is given in equation 5. The energy gap, regardless of how high or low, affects an inhibitor molecule's stability and reactivity.

$$\Delta Eg = ELUMO - EHOMO \qquad (5)$$

Equation 6 is used to determine the proportion of electrons that are transported from the inhibitor to the Fe-surface, or ΔN. One measure that shows this is the molecules' half-electron transfer.

$$\Delta N = \frac{\chi Fe - \chi Inh.}{2(\eta Fe + \eta Inh)} \qquad (6)$$

Back donation of the study was calculated using the relation in the equation 7.

$$\Delta E_{bd} = (\mu^+ - \mu^-)^2 / 4 \, \eta = -\frac{-\eta}{4} \qquad (7)$$

The electron donating (ω⁻) and electron accepting (ω⁺) powers of the molecules has been defined as shown in the equations 8 and 9 [19].

$$\omega^- \approx \frac{(3I+A)^2}{16(I-A)} \qquad (8)$$

$$\omega^+ \approx \frac{(I+3A)^2}{16(I-A)} \qquad (9)$$

With a global hardness (N) of 0eV and a theoretical electronegativity value of (Fe=7.0eV), the metal and molecule were described as accepting and donating using the second order Fukui function (f2), the dual descriptor Δf(k) [2–5]. Equation denotes the difference between the nucleophilic and electrophilic Fukui functions, which is the definition of the second Fukui function. Site K favors an electrophilic assault if f2(r) <0, and a nucleophilic attack if f2(r) > 0. This suggests that the selectivity index f2(r) against electrophilic or nucleophilic assaults functions as an indicator [20].

$$f(k)^+: \text{(for nucleophilic attack)} = \boldsymbol{q}k(N+1) - qk(N) \qquad (10)$$

$$f(k)^-: \text{(for electrophilic attack)} = qk(N) - qk(N-1) \qquad (11)$$

$$f(r) = f^+ \cdot f^- = f^2 \qquad \text{(Fukui function)} \qquad (12)$$

Molecular Dynamics Simulation

A simulation box of 17 x 12 x 28 Å with a periodic boundary condition was used to mimic a representative portion of the surface through calculations utilizing COMPASS FORCEFIELD and Smart ALGORITHM. The Fe crystals were fractionally cleaved at 3.0 Å along the (1 1 1) Plane for Fe. Prior to improving the iron surface and expanding into a 10 × 10 supercell to prevent edge effects, the bottom layers' shape was restricted [1-4]. In order to quench the molecules on the surface, the temperature was set at 350 K. The NVE (microcanonical) ensemble was used to set the temperature, with

a simulation duration of 5 ps and a time step of 1 fs. In order to determine the statistical values of the energies on the surface of Fe (111), the system was programmed to quench every 250 steps [25–29, 22].

To obtain diverse interactions, surfaces and molecules with optimal shapes were employed. Equation 12 was used to compute the Adsorption energy between the inhibitors and the Fe (111) surface. The difference between the total energy of the adsorbates -substrate complex is as coin in equation 12. Binding energy of the simulation was calculated using the equation 13.

$$\text{Adsorption Energy} = E_{total} - (E_{inhibitor} + E_{Fe\ surface}) \tag{13}$$

$$\text{Binding Energy} = -\text{Adsorption energy} \tag{14}$$
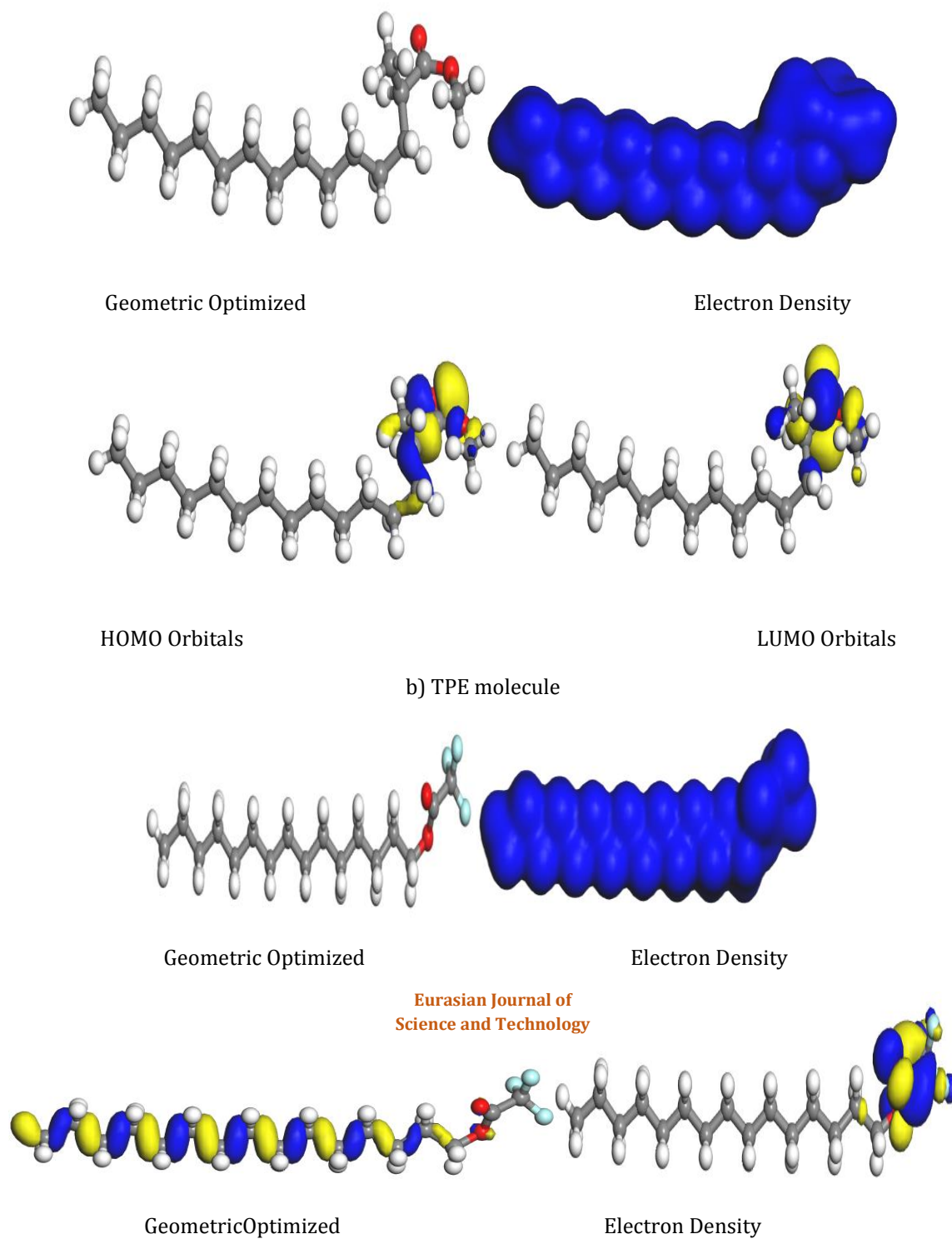
Result and Discussion

Frontier Molecular Orbitals

A molecule's reactivity and selectivity are determined by factors derived from its electronic properties, such as the partial charges on its atoms and electron density, this dependent on the molecule's structure or functional groups present [5-8]. A molecule has many regions that can make the and the metal surface bind together. The ethanoate compounds shown in Figure 2 are the optimized molecules with minimal density energy values of HOMO, and LUMO regions [21]. Regarding the analysis of the outcome-related descriptors, the findings of the calculated values for HOMO and LUMO, respectively, are linked to those obtained using the Ionization energy (I) and Electron Affinity (A) [12]. EHOMO with -I, ELUMO with -A, and their behavior in characterizing the HOMO and LUMO gap relate the three primary descriptors to the simplest conformance to the Koopmans' theorem [17]. The degree of electron transfer from molecules to the empty orbitals of the mild steel (iron) surface is indicated by the maximum value of E_{HOMO} while the lowest E_{LUMO} value in the esters functional group molecules

under study indicates that the molecule with the lowest energy value is more readily capable of receiving electrons from the metal surface than the molecule with the highest E_{LUMO}. In the studied molecules, the increase in E_{HOMO} was in the order of PME>TPE while the E_{LUMO} values were in the TPE>PME. In the course of this research, other descriptors that assess how well the investigated density functionals are beneficial for the prediction of the reactivity of the molecules were also discovered. We refer to this as global reactivity. The stability of the chemical during the reaction is shown by global reactivity descriptors. Considering just the energies of the HOMO and LUMO or the vertical Ionization energy (I) and Electron Affinity (A) for a combination of DFT descriptors, as well as electronegativity (χ), global hardness (η), and global electrophilicity (ω). To confirm the molecule's ability to transmit electrons, the (ΔN) Fraction of Electron transmit and the electron-donating (ω-) and electron-accepting (ω+) powers of the molecules were also computed. According to the optimal molecule's structure, hydrogen is represented by white, nitrogen by red, fluorine by light blue, and carbon by gray.

It is crucial to concentrate on factors that directly affect the inhibitor molecules' electrical interaction with the metal surface when creating a composite index of an inhibitor molecule. These factors consist of half electron transfer (ΔN), Back donation (ΔE_{b-d}), electron donating power (ω-) and electron accepting power (ω+) of the molecules. Others are Dipole moment (Debye), Ionization Potential (I.P), Electron Affinity (EA), Energy gap (ΔE) and electronegativity (χ). From the factors mentioned, the possible stability of the molecules during a specific process is explained by global reactivity (Table 1).

Dipole moments, which account for molecular potential polarity, among the compounds under study revealed that TPE and PME were not electrically stable, that is why their dipole moments do not equal zero (0).

Geometric Optimized   Electron Density

HOMO Orbitals   LUMO Orbitals

b) TPE molecule

Geometric Optimized   Electron Density

GeometricOptimized   Electron Density

Figure 2 geometric optimized molecule, HOMO and LUMO orbitals of the compound and the electron density.

Table 1. The frontier energies of the molecules

Parameters studied	PME	TPE
HOMO (orbital number)	76	88
LUMO (orbital number)	77	89
E_{HOMO} (eV)	-5.018	-6.371
E_{LUMO} (eV)	-0.152	-1.260
Dipole moment (Debye)	1.86	2.17
I.P (eV	5.018	6.371
EA (eV)	0.152	1.260
ΔE(eV)	4.866	5.111
electronegativity(χ)	2.585	3.816
electron transfer(ΔN)	0.907	0.622
ΔE_{b-d} Ev	-0.608	-0.645
(ω^-)	2.969	5.076
(ω^+)	0.384	1.260
ΔN	0.622	0.907

This suggests that, the value of the electron affinity possessed by the molecules, is enough ground to believe that the lowest possible ionization may increase the effectiveness of electron transfer from molecules to the metal surface and vice versa.

Using the computed number of electron transfer (ΔN) of the molecules, this suggested that, the capacity of these inhibitors to donate electrons to the metal surface improves with inhibition efficiency hence the best inhibitor is therefore linked to the largest proportion of electrons transported [10–14].

From the molecules studied, TPE half electron transferred value is grater than that of PME within the range of ($\Delta N<3.6$) suggesting that, inhibition efficiency of the molecules depends on the number of the electron transferred but not only by the size of the molecules [26,29].

The electron donor and acceptor power determined by calculating the values of the molecules showed that a system with a higher $\omega+$ value is more capable of receiving charges, while a system with a lower $\omega-$ value is more suitable for donating electrons. The molecules followed the trend based on the computed values that were obtained [18].

The difference between a molecule's LUMO and HOMO energies is known as the energy gap [10–15]. A slower potential for electron transport between atoms inside molecules is indicated by a greater discrepancy between LUMO and HOMO values [9–13]. The investigated compounds' reduced energy gap demonstrates their enormous potential. The molecules' energy gaps were in the order of TPE> PME. This demonstrates that PME inhibitor, in comparison to TPE inhibitor will be more effective in slowing the corrosion process on the metal surface base on the lower value of the energy gap presented. Also, TPE is more stable inhibitor compare to PME molecule and will be more reactive in preventing corrosion activities on the metal surface.

Fukui Functions

The relative reactivity of each atomic site in the molecule may be explained using Fukui functions, a measure of local reactivity [1]. Because there are many substituted hetero-atoms in the molecule, the condensed Fukui Function and local reactivity indices allow for the description of the various molecular components based on their distinct chemical behaviors [7]. Descriptors called Fukui indices can be used to identify an assault as being radical, electrophilic, nucleophilic, or any

combination of these [10]. The atoms with the highest negative charge densities are thought to have the most potentially reactive locations for molecule adsorption. Gaining knowledge about the active locations for the compounds' possible radical assault is interesting given the possible use of the investigated molecules as inhibitors. The condensed dual descriptor's estimated findings using both f^2 Mulliken (M) and f^2 Hirshfield (H) atomic charges were provided. As shown in Table 2-3 for the molecules. the electrophilic and nucleophilic Parr functions with Hirshfeld atomic spin densities $Pk^+(H)$ and $Pk^-(H)$ are the electrophilic and nucleophilic Parr functions with Mulliken atomic spin densities $Pk^+(M)$ and $Pk^-(M)$. The result of the local reactivity descriptors in Table 3-4, concluded that C1, O3,

O4 and C23 will be the preferred sites for a nucleophilic attack and that the atoms will act as electrophilic sites for a nucleophilic attack in the PTE molecule [8]. H40 and H4 are examples of compounds that are attacked electrophilically. The second Fukui function (dual descriptor) generally showed that the molecule TPE has a greater propensity for nucleophilic assault, thus $f^2(M)$ and $f^2(H)$ had positive values in contrast to the negative and zeros, which denote electrophilic and radical attacks, respectively [15]. The second molecule PME exhibits a similar pattern, with O16 having the greatest value for both nucleophilic and electrophilic properties. This suggests that O16 has the ability to both donate and take electrons from the mild steel surface [12].

Table 2 The fukui functions of the pte molecule

Atom	P_k^+(M)	P_k^+(H)	P_k^-(M)	P_k^-(H)	f^2(M)	f^2(H)
C (1)	0.227	0.217	0.004	0.009	0.223	0.208
C (2)	0.063	0.057	0.001	0.002	0.062	0.055
O (3)	0.232	0.226	0.023	0.027	0.209	0.199
O (4)	0.109	0.115	0.018	0.014	0.091	0.101
F (5)	0.063	0.059	0.009	0.005	0.054	0.054
F (6)	0.065	0.073	0.008	0.007	0.057	0.066
F (7)	0.065	0.073	0.01	0.01	0.055	0.063
C (8)	-0.053	0.018	0.001	0.006	-0.054	0.012
C (9)	-0.024	0.005	0.012	0.008	-0.036	-0.003
C(10)	-0.01	0.006	0.008	0.013	-0.018	-0.007
C(11)	-0.009	0.003	0.009	0.017	-0.018	-0.014
C(12)	-0.011	0.003	0.006	0.023	-0.017	-0.02
C(13)	-0.005	0.002	0.011	0.028	-0.016	-0.026
C(14)	-0.005	0.001	0.01	0.033	-0.015	-0.032
C(15)	-0.005	0.001	0.01	0.037	-0.015	-0.036
C(16)	0.00	0.001	0.014	0.039	-0.014	-0.038
C(17)	-0.001	0.001	0.014	0.039	-0.015	-0.038
C(18)	0.002	0.001	0.015	0.038	-0.013	-0.037
C(19)	-0.004	0	0.01	0.035	-0.014	-0.035
C(20)	0.001	0.001	0.014	0.031	-0.013	-0.03
C(21)	-0.006	0.001	0.008	0.025	-0.014	-0.024
C(22)	0.002	0.001	0.017	0.024	-0.015	-0.023

Table 3 The fukui functions of the pme molecule

| Atom	P_k^+(M)	P_k^+(H)	P_k^-(M)	P_k^-(H)	f^2(M)	f^2(H)
C (1)	0.263	0.216	0.058	0.102	0.205	0.114
C (2)	-0.08	0.048	-0.003	0.009	-0.077	0.039
C (3)	0.021	0.008	-0.071	0.021	0.092	-0.013
C (4)	-0.019	-0.005	-0.004	0.022	-0.015	-0.027
C (5)	0.019	0.003	-0.058	0.003	0.077	0.000
C (6)	-0.013	0.000	0.00	0.009	-0.013	-0.009
C (7)	-0.016	-0.007	0.006	0.009	-0.022	-0.016
C (8)	0.004	0.011	-0.012	-0.006	0.016	0.017
C (9)	-0.001	0.003	-0.004	-0.001	0.003	0.004
C(10)	-0.023	0.007	0.017	-0.004	-0.04	0.011
C(11)	0.000	0.005	-0.003	-0.004	0.003	0.009
C(12)	-0.02	0.008	0.016	-0.007	-0.036	0.015
C(13)	-0.009	0.007	0.007	-0.007	-0.016	0.014
C(14)	0.02	0.007	-0.023	-0.006	0.043	0.013
C(15)	-0.034	0.009	0.031	-0.007	-0.065	0.016
O(16)	0.148	0.202	0.468	0.388	-0.32	-0.186
O(17)	0.097	0.069	0.053	0.116	0.044	-0.047
C(18)	-0.134	0.051	0.07	-0.001	-0.204	0.052
C(19)	-0.104	0.017	0.013	0.043	-0.117	-0.026

Molecular Dynamic Simulation

A method devised to investigate the possible mechanism of chemical reactions that lead to molecule-to-surface interactions on metal surfaces for inhibition is called "compound simulation on metal surfaces" [19–24]. stating the expected response and its potential viability in a real-world scenario. A thorough of understanding of the protective inhibitor molecule's interaction with the metal surface is necessary to clarify the inhibition mechanism [10]. Fe (110) crystal surface was constructed in this context in order to investigate the nature of inhibition of two molecules, TPE and PME. This is due to the fact that Fe (110) is one of the iron surfaces that has a high surface coverage and density [12]. In mild steel alloys that are positively charged in relation to the potential of zero charge (PZC) in solution, iron makes up the majority of the metal content—roughly 90% [2] (Figures 3a, 3b).
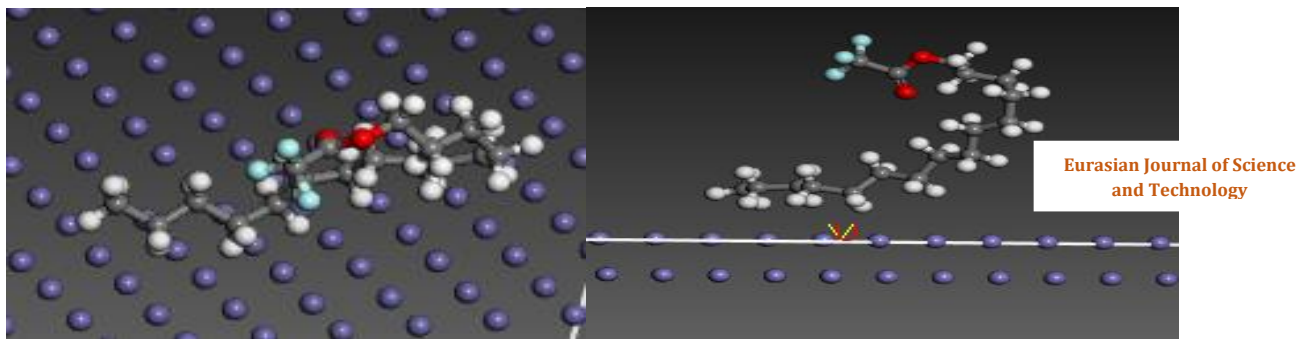
Figure 3a The snap short of PTE on the surface of mild steel
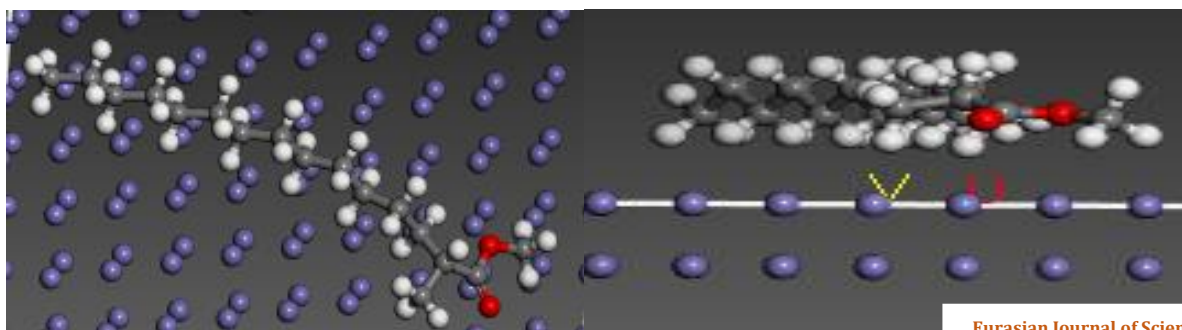
Figure 3b The snap short of PME on the surface of mild steel

Table 4 Present adsorption energy obtained from the computational simulation of the molecules PME and TPE

Properties (kJ.mol^{-1})	TPE	PME
Total Potential Energy	-549.464±2.3	-986.887±17
Energy of the Molecule	-175.377±2.1	-373.978±0.0
Energy of Fe (110)	0.000 ±0.0	0.000 ±0.0
Adsorption energy	-374.087±2.2	-312.909±8.5
Binding energy	374.087±2.2	312.909±8.5

Following QSAR analysis at 350K, Table 4 showed the energy of the inhibition on the surface of Fe (110). Strong chemisorption with enough energy is confirmed by the size of the adsorption energy obtained, which was greater than the threshold value of 40 kJ/mol [17–20]. This is the inhibition of the TPE and PME molecules, which were best explained by their chemical behavior together with the mild steel

Conclusion

Based on the investigation, the DFT quantum chemical technique was used to explore the molecules TPE and PME for the inhibitory efficiency on mild steel Fe (110). Based on the inhibition process's binding and adsorption energies, it can be concluded that both compounds' inhibition process included a greater degree of chemisorption mechanism. The number of electron transfer (ΔN) value of iron indicates that electron transfer was the driving force behind the inhibitory process.

Both of the molecules' Fukui values indicate that they have a lot of potential and that their hetero-atom functional group delocalization on the surfaces contributed to their adsorptive strength. The larger percentage of positive values reported on the acquired f^2 value indicates that all of the molecules were more donor agents on the mild steel surface, as explained by the second fukui function.

Conflict of Interest

The authors declare no conflict of interest.

Acknowledgments

ORCID

Abdullahi Muhammad Ayuba
https://www.orcid.org/0000-0002-2295-8282
Thomas Aondofa Nyijime
https://www.orcid.org/0000-0001-9537-1987
Safiyya Abubakar Minjibir
https://www.orcid.org/0009-0006-4671-2670
Fater Iorhuna
https://www.orcid.org/0000-0002-1018-198X

References

[1] AlMashhadani H.A., Saleh K.A., Electrochemical Deposition of Hydroxyapatite Co-Substituted By Sr/Mg Coating on Ti-6Al-4V ELI Dental Alloy Post-MAO as Anti-Corrosion, *Iraqi Journal of Science*, 2020, 2751-2761 [Crossref], [Google Scholar], [Publisher]

[2] Afandiyeva L., Abbasov V., Aliyeva L., Ahmadbayova S., Azizbeyli E., El-Lateef Ahmed H.M., Investigation of organic complexes of imidazolines based on synthetic oxy-and petroleum acids as corrosion inhibitors, *Iranian Journal of Chemistry and Chemical Engineering*, 2018, **37**:73 [Crossref], [Google Scholar], [Publisher]

[3] Jafari H., Mohsenifar F., Sayin K., Effect of alkyl chain length on adsorption behavior and corrosion inhibition of imidazoline inhibitors, *Iranian Journal of Chemistry and Chemical Engineering (IJCCE)*, 2018, **37**:85 [Crossref], [Google Scholar], [Publisher]

[4] Elmi S., Foroughi M.M., Dehdab M., Shahidi-Zandi M., Computational evaluation of corrosion inhibition of four quinoline derivatives on carbon steel in aqueous phase, *Iranian Journal of Chemistry and Chemical Engineering (IJCCE)*, 2019, **38**:185 [Crossref], [Google Scholar], [Publisher]

[5] Noorollahy Bastam N., Hafizi-Atabak H.R., Atabaki F., Radvar M., Jahangiri S., Electrochemical Measurements for the Corrosion Inhibition of Mild steel in 0.5 M HCl Using poly (epichlorohydrin) Derivatives, *Iranian Journal of Chemistry and Chemical Engineering*, 2020, **39**:113 [Google Scholar], [Publisher]

[6] Popoola L.T., Aderibigbe T.A., Lala M.A., Mild Steel Corrosion Inhibition in Hydrochloric Acid Using Cocoa Pod Husk-Ficus exasperata: Extract Preparation Optimization and Characterization, *Iranian Journal of Chemistry and Chemical Engineering*, 2022, **41**:482 [Crossref], [Google Scholar], [Publisher]

[7] Kubba R.M., Al-Joborry N.M., Theoretical study of a new oxazolidine-5-one derivative as a corrosion inhibitor for carbon steel surface, *Iraqi Journal of Science*, 2021, 1396 [Crossref], [Google Scholar], [Publisher]

[8] Al-Rudaini K.A.K., Al-Saadie K.A.S., Milk Thistle Leaves Aqueous Extract as a New Corrosion Inhibitor for Aluminum Alloys in Alkaline Medium, *Iraqi Journal of Science*, 2021, 363 [Crossref], [Google Scholar], [Publisher]

[9] Mohammed M.A., Kubba R.M., Experimental Evaluation for the Inhibition of Carbon Steel Corrosion in Salt and Acid Media by New Derivative of Quinolin-2-One, Iraqi Journal of Science, 2020, 1861 [Crossref], [Google Scholar], [Publisher]

[10] Mammeri S., Chafai N., Harkat H., Kerkour R., Chafaa S., Protection of steel against corrosion in acid medium using dihydropyrimidinone derivatives: experimental and DFT study, *Iranian Journal of Science and Technology, Transactions A: Science*, 2021, **45**:1607 [Crossref], [Google Scholar], [Publisher]

[11] Orokpo A.M., Wuana R.A., Chuhul H.F., Eneji I.S., Corrosion Inhibition Potential of Benue Propolis Extracts on Carbon Steel in 1.0 M Hydrochloric Acid Medium: Experimental and Computational Studies. *Progress in Chemical and Biochemical Research*, 2022, **5**:283 [Crossref], [Google Scholar], [Publisher]

[12] Esan T., Oyeneyin O., Olanipekun A., Ipinloju N., Corrosion inhibitive potentials of some amino acid derivatives of 1, 4-naphthoquinone–DFT calculations, *Advanced*

Journal of Chemistry-Section A, 2022, **5**:263 [Crossref], [Google Scholar], [Publisher]

[13] Kubba R.M., Al-Joborry N.M., Al-Lami N.J., Theoretical and experimental studies for inhibition potentials of imidazolidine 4-one and oxazolidine 5-one derivatives for the corrosion of carbon steel in Sea Water, *Iraqi Journal of Science*, 2020, 2776 [Crossref], [Google Scholar], [Publisher]

[14] Yavari Z., Darijani M., Dehdab M., Comparative theoretical and experimental studies on corrosion inhibition of aluminum in acidic media by the antibiotics drugs. Iranian Journal of Science and Technology, Transactions A: Science, 2018, **42**:1957 [Crossref], [Google Scholar], [Publisher]

[15] Al-Joborry N.M., Kubba R.M., Theoretical and Experimental Study for Corrosion Inhibition of Carbon Steel in Salty and Acidic Media by A New Derivative of Imidazolidine 4-One, *Iraqi Journal of Science*, 2020, 1842 [Crossref], [Google Scholar], [Publisher]

[16] Adebayo O.L., Esan T.O., Organic Constituents in Air-Dried Alchornea laxifloral Leaves (AALL) Extract: Corrosion Remediation, Isolation and Structural Elucidation. *Advanced Journal of Chemistry, Section A.* 2023, **6**:225 [Crossref], [Google Scholar], [Publisher]

[17] Belghiti M.E., Echihi S., Dafali A., Karzazi Y., Bakasse M., Elalaoui-Elabdallaoui H., Olasunkanmi L.O., Ebenso E.E., Tabyaoui M., Computational simulation and statistical analysis on the relationship between corrosion inhibition efficiency and molecular structure of some hydrazine derivatives in phosphoric acid on mild steel surface, *Applied surface science*, 2019, **491**:707 [Crossref], [Google Scholar], [Publisher]

[18] Kadhim M.M., Juber L.A.A., Al-Janabi A.S., Estimation of the Efficiency of Corrosion Inhibition by Zn-Dithiocarbamate Complexes: a Theoretical Study, *Iraqi Journal of Science*, 2021, 3323 [Crossref], [Google Scholar], [Publisher]

[19] Glossman-Mitnik D., Computational study of the chemical reactivity properties of the Rhodamine B molecule, *Procedia Computer Science*, 2013, **18**:816 [Crossref], [Google Scholar], [Publisher]

[20] Nahlé A., Salim R., El Hajjaji F., Aouad, M.R., Messali M., Ech-Chihbi E., Hammouti B., Taleb M., Novel triazole derivatives as ecological corrosion inhibitors for mild steel in 1.0 M HCl: experimental & theoretical approach. *RSC advances*, 2021, **11**:4147 [Crossref], [Google Scholar], [Publisher]

[21] Eddy N.O., Ameh P.O., Essien N.B., Experimental and computational chemistry studies on the inhibition of aluminium and mild steel in 0.1 M HCl by 3-nitrobenzoic acid, *Journal of Taibah University for Science*, 2018, **12**:545 [Crossref], [Google Scholar], [Publisher]

[22] Guo L., Zhu M., Chang J., Thomas R., Zhang R., Wang P., Zheng X., Lin Y., Marzouki R., Corrosion Inhibition of N80 Steel by Newly Synthesized Imidazoline Based Ionic Liquid in 15% HCl Medium: Experimental and Theoretical Investigations, *International Journal of Electrochemical Science*, 2021, **16**:211139 [Crossref], [Google Scholar], [Publisher]

[23] Lgaz H., Masroor S., Chafiq M., Damej M., Brahmia A., Salghi R., Benmessaoud M., Ali I.H., Alghamdi M.M., Chaouiki A., Chung I.M., Evaluation of 2-mercaptobenzimidazole derivatives as corrosion inhibitors for mild steel in hydrochloric acid, *Metals*, 2020, **10**: 357 [Crossref], [Google Scholar], [Publisher]

[24] Iorhuna F., Thomas N.A., Lawal S.M., A Theoretical properties of Thiazepine and its derivatives on inhibition of Aluminium Al (110) surface, *Algerian Journal of Engineering and Technology*, 2023, **8**:43 [Crossref], [Google Scholar], [Publisher]

[25] Kılınççeker G., Baş M., Zarifi F., Sayın, K., Experimental and Computational Investigation for (E)-2-hydroxy-5-(2-benzylidene) Aminobenzoic Acid Schiff Base as a Corrosion

Inhibitor for Copper in Acidic Media. *Iranian Journal of Science and Technology, Transactions A: Science*, 2021, **45**: 515 [Crossref], [Google Scholar], [Publisher]

[26] Nyijime T., Chahul H., Ayuba A., Iorhuna F., Theoretical investigations on thiadiazole derivatives as corrosion inhibitors on mild steel, *Advanced Journal of Chemistry-Section A,* 2023, **6**: 141 [Crossref], [Google Scholar], [Publisher]

[27] Ogunyemi B.T., Latona D.F., Ayinde A.A., Adejoro I.A.,Theoretical Investigation to Corrosion Inhibition Efficiency of Some Chloroquine Derivatives Using Density Functional Theory. *Advanced Journal of Chemistry, Section A*, 2020, **3**: 485 [Crossref], [Google Scholar], [Publisher]

[28] Iorhuna F., Ayuba A.M., Nyijime T.A., Muhammmedjamiu H., A DTF and Molecular thermodynamic Simulation on the Adsorption Inhibition of Cytarabine a Nucleotides as a Potential Inhibitor on the Alumnium Metal Surface. *Eurasian Journal of Science and Technology*, 2023, **3**:4 [Crossref], [Google Scholar], [Publisher]

[29] Edachea E.I., Dawia H.A., Ugbeb F.A., Dynamics Simulations and Structural Studies of Some Selected Inhibitors of the Glycoprotein (GPC) of Lassa Virus, *Journal of Applied Organometallic Chemistry*, 2023, **3**:224 [Crossref], [Google Scholar], [Publisher]